REFINED RFP LOOP VOLTAGE CALCULATION

J.C. Sprott

PLP 1053

April 1989

Plasma Studies

University of Wisconsin

Refined RFP Loop Voltage Calculation

J. C. Sprott

I. Introduction

A critical figure-of-merit for RFP devices is the loop voltage. Low loop voltage implies high plasma temperature and long energy confinement time. In simplest form, the loop voltage is obtained from the voltage induced in a single-turn toroidal loop at the plasma surface, and hence its name. For more careful work, it is necessary to correct the voltage thus obtained for a number of effects.

To begin with, the measured voltage in general depends on the poloidal location of the loop since the plasma surface may not be a surface of constant flux, especially in an air-core machine with a highly resistive confining shell or with an internal limiter or resistive liner. In some experiments, a number of loops are placed around the plasma at different poloidal locations and connected in series, and the loop voltage is obtained by dividing the measured voltage by the number of turns. In a device such as MST with a highly conducting shell, the plasma surface closely approximates a flux surface except for small soak-in effects and field errors at the poloidal gap, and hence all loops at the plasma surface will give nearly identical results. We will hereafter reserve the term "surface

voltage" for the voltage measured in this way.

It is often convenient to place the loop outside the vacuum liner, and, in some cases, also outside the conducting shell (which in MST is the same as the vacuum liner). In such a case it is necessary to correct for the flux between the surface on which the loop measures and the plasma surface in order to calculate the surface voltage. The correction is smallest if the loop is as close to the outside of the shell and as far from the primary windings as possible.

If the plasma is in steady state (constant plasma current, constant toroidal magnetic flux, constant plasma internal energy, and constant magnetic field profile), the surface voltage measurement as described above, along with a measurement of the total toroidal plasma current, would suffice to determine the ohmic input power (from the product) and plasma resistance (from the ratio). With additional assumptions and/or measurements, the energy confinement time and plasma temperature can be deduced from the input power and resistance. If the plasma is not in steady-state, the required corrections can be large.

The purpose of this note is to examine more critically the necessary corrections and to refine the presently used formula from which the loop voltage in MST is calculated from the measured quantities (as described in PLP 1039).

II. Generalized Definition of Loop Voltage

A convenient starting point is the equation for energy balance of the plasma,

$$V_\phi I_p + V_\theta I_t = dU_m/dt + dU_p/dt + U_p/\tau_E \tag{1}$$

where V_ϕ is the surface voltage in the toroidal direction, V_θ is the surface voltage in the poloidal direction, I_p is the net plasma current encircling the toroid, I_t is the net current in the toroidal field circuit piercing the hole in the toroid, U_m is the stored magnetic energy, U_p is the plasma energy, and τ_E is the global energy confinement time, which is in effect defined by the above equation and is generally the unknown for which Eq. (1) is solved.

A reasonable and convenient generalization is to define the loop voltage V_ℓ such that τ_E is simply given by

$$V_\ell I_p = U_p/\tau_E \tag{2}$$

which when combined with Eq. (1) gives

$$V_\ell = V_\phi + V_\theta I_t/I_p - dU/dt/I_p \tag{3}$$

where

$$U = U_m + U_p = \int (B^2/2\mu_o + 3p/2)\, dV \tag{4}$$

B is the magnetic field, p is the plasma pressure (assumed isotropic),

and the integral is over of the plasma volume.

The loop voltage evaluated as in Eq. (3) is sometimes called the "resistive voltage" since it is the voltage that must be multiplied by the plasma current to get the ohmic input power to the plasma. The resistive voltage is sometimes defined to exclude the dU_p/dt term which is smaller than dU_m/dt by a factor of the order of the plasma beta. Our definition is preferred because it leads to a simpler evaluation of τ_E and because U is more nearly constant than either U_m or U_p since an increase in U_p results in a diamagnetic decrease in U_m.

III. Correction for Wall Flux Soak-in

Assume that the loop used to measure the toroidal voltage is separated from the plasma surface by a conductor of resistivity ρ, permeability μ_o and thickness d and that the field just outside the conductor is negligible compared with the field inside. The externally measured voltage will be denoted by V_{pg} in accordance with local convention since it is the voltage drop across the poloidal gap as measured from outside the vacuum. The voltage difference $V_{pg} - V_\phi$ is due to the time-derivative of the poloidal flux that has soaked into the wall. As described by Kerst and Sprott [J. Appl. Phys. 60, 475 (1986)], this correction can be represented in the plane approximation as the voltage drop across the R-L network shown in Fig. 1, the low-frequency limit of which is given by

$$V_\phi = V_{pg} - I_p R_w - L_w dI_p/dt \qquad (5)$$

where in the large aspect ratio (R_o/a) limit, R_w and L_w are given by

$$R_w = R_o \rho/ad \quad \text{and} \quad L_w = \mu_o R_o d/3a \qquad (6)$$

Note that this calculation is appropriate only up until the time at which significant field begins to soak through the wall. In the truly dc limit, the wall current resistively decays to zero and no correction is required. Thus a more proper calculation requires one to measure the wall current and to use its value in place of I_p in Eq. (5). A similar correction would be required for determining V_θ from the toroidal flux loop V_{tg} (using values of L and R smaller than those in Fig. 1 by a factor of a^2/R_o^2) except for the fact that the toroidal flux loop is inside the vacuum vessel in MST.

IV. Representation in Terms of Measured Quantities

An exact evaluation of Eq. (3) requires a measurement of the magnetic field and plasma pressure profiles. Such measurements are difficult, and thus it is usually necessary to invoke some model (such as the Bessel function model of Taylor) to calculate the required terms from easily measured quantities such as Φ_t, I_p and I_t. Fortunately, there is considerable experimental evidence that RFP plasmas tend to relax to a unique magnetic field profile and beta that can be characterized by any two of the above three quantities. Choosing Φ_t

and I_p as the state variables, Eq. (3) can be written in the form

$$V_\ell = V_\phi - LdI_p/dt - AV_\theta \tag{7}$$

where

$$L = \frac{1}{I_p}\frac{\partial U}{\partial I_p}\bigg|_{\Phi_t=\text{const}} \tag{8}$$

and

$$A = \frac{1}{I_p}\frac{\partial U}{\partial \Phi_t}\bigg|_{I_p=\text{const}} - \frac{I_t}{I_p} \tag{9}$$

In Eq. (9) use has been made of the fact that $V_\theta = d\Phi_t/dt$.

The quantity L has dimensions of inductance, and the quantity A is a dimensionless number that we will hereafter refer to as the coupling coefficient since it describes the coupling of the toroidal and poloidal field circuits. In accordance with the above, there is reason to hope that L and A can be expressed in terms of either θ or F as given by

$$\theta = \mu_o I_p a/2\Phi_t \tag{10}$$

and

$$F = \mu_o I_t a^2/2R_o\Phi_t \tag{11}$$

The extent to which L and A can be expressed as functions of θ independent of the chosen model will be the subject of much of the

remainder of this note.

V. Prediction of the Polynomial Function Model

The calculation of the loop voltage in MST has to date made use of the polynomial function model (PFM) [described in Phys. Fluids 31, 2266 (1988)]. The polynomial function model has the virtue of agreeing with the Bessel function model (constant j/B) near the axis, but with j falling smoothly to zero at r=a as in the modified Bessel function model and as observed in experiment. B and j are given by analytic functions of r, facilitating calculation, and a small perpendicular current is allowed, corresponding to a value of beta close to that experimentally observed. The predicted F-θ curve agrees as well with experiment as does any of the many other models in common use.

The polynomial function model leads to a prediction of L(θ) and A(θ) which are well fit by the functions:

$$L \approx 9\mu_o R_o(2+3\theta^2) \;/\; 8(6+\theta^2) \tag{12}$$

and

$$A \approx 4R_o\theta(1-\theta^2) \;/\; a(8+3\theta^3) \tag{13}$$

VI. Comparison with Loop Voltage on Axis

Before proceeding to examine the sensitivity of L and A to the assumed model, it is instructive to digress to comment on the relation between the loop voltage defined by Eq. (3) and the voltage (V_o) that would be measured by a loop placed on the plasma axis:

$$V_o = V_\phi - d\Phi_p/dt \tag{14}$$

where in the cylindrical approximation the poloidal flux Φ_p is

$$\Phi_p = 2\pi R_o \int_o^a B_p \, dr \tag{15}$$

V_o can be written in a form analogous to Eq. (7):

$$V_o = V_\phi - L'dI_p/dt - A'V_\theta \tag{16}$$

where

$$L' = \left.\frac{\partial \Phi_p}{\partial I_p}\right|_{\Phi_t=\text{const}} \tag{17}$$

and

$$A' = \left.\frac{\partial \Phi_p}{\partial \Phi_t}\right|_{I_p=\text{const}} \tag{18}$$

The comparison of L' from Eq. (17) and L from Eq. (8) as predicted by the polynomial function model is shown in Fig. 2, and the comparison of A' from Eq. (18) and A from Eq. (9) as predicted by the polynomial model is shown in Fig. 3.

The loop voltage on axis calculated from Eq. (16) can be combined

with a model of the toroidal current profile to calculate the resistivity on axis from which the axis conductivity temperature can be derived. With an independent measure of the temperature on axis, say, from Thomson scattering, the axis value of the effective ionic charge Z_{eff} can be deduced.

VII. Sensitivity to Profiles

Although the polynomial function model gives reasonable agreement with experiment, it is not perfect, especially during the rapid relaxation events commonly referred to as "sawteeth" or "flux jumps," during which the excursion in F-θ space tends to be orthogonal to the F-θ trajectory that the plasma follows on a slower time scale. A typical example of such behavior in MST is shown in Fig. 4. In order to allow for departures from a unique trajectory in F-θ space, it is necessary to consider a family of profiles characterized by at least two parameters, the variation of which can be mapped into the region of F-θ space accessed by experiment.

The calculation proceeds in the usual way, starting with Ampere's law,

$$\nabla \times \underline{B} = \mu_o \underline{j} \tag{19}$$

with the current density $\underline{j}$ given by the equilibrium condition,

$$\underline{j} = \underline{j}_{||} + \underline{B} \times \nabla p \; / \; B^2 \tag{20}$$

which can be combined into a single differential equation for $\underline{B}$:

$$\nabla \times \underline{B} = \lambda \underline{B} + \mu_o \underline{B} \times \nabla p / B^2 \tag{21}$$

Eq. (21) is solved numerically in the axisymmetric, cylindrical approximation with a parabolic pressure profile,

$$p = p_o(1-r^2/a^2) \tag{22}$$

In such a case Eq. (21) breaks down into two, coupled, first order differential equations for the toroidal and poloidal fields:

$$\partial B_t/\partial r = -\lambda B_p + \beta r B_t B_{to}{}^2/a^2 B^2 \tag{23}$$

and

$$\partial(rB_p)/\partial r = \lambda r B_t + \beta r^2 B_p B_{to}{}^2/a^2 B^2 \tag{24}$$

where

$$B = [B_t{}^2 + B_p{}^2]^{1/2} \tag{25}$$

and

$$\beta = 2\mu_o p_o \; / \; B_{to}{}^2 \tag{26}$$

is the plasma beta on axis, and λ is an arbitrary function of r. Eqs. (23) and (24) have been solved for various values of $\lambda(r)$ and β.

A case which has been often used, and with some experimental justification, is the so-called modified Bessel function model (MBFM) with $\beta=0$ in which λ is taken to be constant (λ_o) for $r/a < b$ and linearly decreasing to zero at $r/a = 1$. Thus λ_o and b become the two parameters whose variation can be mapped into F-θ space as shown in Fig. 5. The b=1 limit represents the Taylor Bessel function model (BFM). The numerical result can be fit reasonably well to a function of the form

$$F \approx 1 - \theta^2/2 + (1-4b^3)\theta^4/24 \qquad (27)$$

To calculate the loop voltage, we return to the basic definition given in Eq. (3) in which the energy U plays an important role. For the MBFM, U is a function of three variables in the calculation, B_{to}, λ_o and b which are mapped into F-θ space and displayed as normalized contours of constant U in Fig. (6). An important feature of Fig. (6) is that in the region of interest the energy depends primarily on θ and only weakly on F for a given θ. Thus the choice of expressing the inductance given by Eq. (8) as a function of θ rather than F in Eq. (12) was serendipitous. Stated differently, the plasma inductance, when expressed as a function of θ is not sensitively dependent on the shape of the λ profile, and thus the value derived from the polynomial function model is probably as good a representation as any.

Similarly, the coupling coefficient given by Eq. (9) has a term involving $\partial U/\partial \Phi_t$ at constant I_p and is thus primarily a function of θ. However, the second term on the right of Eq. (9) is exactly $R_o F/a\theta$. In the polynomial function model, F is given in terms of θ approximately by

$$F \approx 1 - \theta^2/2 \tag{28}$$

and thus it is possible to express this term as a function of θ alone. However, it is not necessary to do so since F is an easily measured quantity in the experiment. Rather than recalculate the PFM result, one can simply replace the value predicted therefrom with the following:

$$A \longrightarrow A + R_o(1-\theta^2/2-F) \;/\; a\theta \tag{29}$$

The correction term is obviously zero if F follows the form of Eq. (28) but allows for some departure from the PFM result. Note that there is a singularity in the correction term at $\theta=0$, and so if F is not precisely 1.0 at $\theta=0$, the correction will diverge. Thus it is probably best to apply the correction only above some value of θ such as $\theta=1$ at which A=0 in the PFM or perhaps only for F<0. For the worst case in Fig. 4 ($\theta=1.9$), the correction amounts to about 50%.

The extent to which the above results are altered by finite beta was tested by repeating the calculation with $\beta=10\%$ on axis,

corresponding to $\beta_p \sim$ 30-50% for F<0, where β_p is defined by

$$\beta_p = 8\pi^2 a^2 p_o / \mu_o I_p^2 \tag{30}$$

This value is somewhat higher than typically observed in RFP's and thus presumably brackets the interesting range of parameters. The resulting F-θ curves are shown in Fig. 7, and the contours of constant energy are shown in Fig. 8. The results are qualitatively similar to the β=0 case, and, in fact, the constant energy contours are even less sensitive to variations in F at a given θ. Many other λ-profiles have been examined with similar results.

VIII. An Improved Formalism

If the plasma is permitted to move arbitrarily in F-θ space rather than follow a unique trajectory, a correct solution requires that the problem be reformulated to allow the energy U to be a function of three variables (I_p, Φ_t, and I_t) rather than two (I_p and Φ_t). In such a case, the generalization of Eq. (7) is

$$V_\ell = V_\phi - L'' dI_p/dt - A'' V_\theta - M'' dI_t/dt \tag{31}$$

where

$$L'' = \frac{1}{I_p} \frac{\partial U}{\partial I_p} \tag{32}$$

and

$$A'' = \frac{1}{I_p}\frac{\partial U}{\partial \Phi_t} - \frac{I_t}{I_p} \tag{33}$$

and

$$M'' = \frac{1}{I_p}\frac{\partial U}{\partial I_t} \tag{34}$$

Although Eqs. (32) and (33) look identical to Eqs. (8) and (9), they are very different in that the partial derivatives are taken holding two things constant rather than one. Thus the values of L" and A" above are different from and should not be confused with the L and A used previously. Furthermore, Eq. (34) defines a new quantity M" which we will call the mutual inductance since it has dimensions of inductance and involves a coupling between the toroidal and poloidal-field circuits. From Eq. (28), the following relations which are valid for the PFM can be obtained:

$$L \approx L'' - R_o \theta M''/a \tag{35}$$

and

$$A \approx A'' + R_o(2+\theta^2)M''/\mu_o a^2 \tag{36}$$

Normalized values for U, L", A" and M" for the MBFM with $\beta=0$ have been calculated numerically. Since each quantity is a function of two variables (F and θ), no attempt has been made to plot the results, but a table of numerical values is included in Fig. 9. The functional dependence is complicated, but a bi-linear expansion about a typical

operating point of F=-0.2 and θ=1.6 gives

$$L''/\mu_o R_o \approx 2.6\theta + 1.2F - 2.0 \tag{37}$$

$$aA''/R_o \approx 7.5 - 6.3\theta - 3.3F \tag{38}$$

$$M''/\mu_o a \approx 2.2\theta + 1.3F - 3.1 \tag{39}$$

Expressions of this type would be useful for calculating the loop voltage variation during a sawtooth oscillation under the assumption that the trajectory in F-θ space is a consequence of a profile rather than a pressure readjustment. Note that to apply Eq. (31) it is necessary to generate a suitably smoothed signal proportional to dI_t/dt.

IX. A Comment on Minimum Energy States

Before concluding, it is worth pointing out a curious and perhaps significant feature of the variation of energy with F and θ. Magnetic field profiles in an RFP are generally assumed to relax to a shape that represents a state of minimum total energy subject to whatever constraints are present. In the Taylor (BFM) model, the constraints are taken to be toroidal flux Φ_t and total magnetic helicity K. In an experiment, one instead generally relies on the external circuit to constrain the toroidal flux and the plasma current I_p (so called "flat-topped operation"). In such a case, the helicity would be expected to

readjust on a shorter resistive time scale. Constraining I_p and Φ_t is equivalent to specifying θ and letting the plasma relax to whatever value of F minimizes the energy. If one further constrains the profile to be given by the modified Bessel function model (with adjustable b) and $\beta=0$, inspection of Fig. 6 shows that for $F>0$, the minimum energy state (at constant θ) is the BFM (b=1), but for $F<0$ (RFP-like), the minimum energy state lies to the right of the BFM curve as seen in experiment. Fig. 10 shows the locus of minimum energy states for this case along with a similar calculation in which helicity is conserved rather than plasma current (reproducing the BFM result). Thus for a given θ, the MBFM is a lower energy state than the BFM in an RFP.

Adding finite beta to the MBFM does not qualitatively change the result as shown in Fig. 11 for a parabolic pressure profile with a beta on axis of 10%. From similar plots with various beta, the minimum energy state of the MBFM for constant I_p and $F<0$ is quite accurately given by

$$F \approx 1/(1+3.8\beta) - \theta/(1.2+6\beta) \qquad (40)$$

A large number of other lambda profiles have been examined with similar results. Even a case in which lambda is a delta function of position, $\lambda = \lambda_o \delta(b-r/a)$, in which λ_o and b are varied to access different regions of F-θ space gives a similar result. In the latter case, the minimum energy state for $\theta \leqq 1$ has b=1 and follows the curve

$$F = [1 - \theta^2]^{1/2} \qquad (41)$$

but for $\theta>1$, the minimum energy requires $b<1$ and occurs for F slightly negative. Thus it is possible that the experimentally observed F-θ curve is a consequence of the constraints imposed externally by the circuit that drives the RFP rather than by any considerations of helicity conservation. This possibility will be examined further in a forthcoming paper.

X. Conclusions

A number of subtleties have been examined concerning the way in which loop voltage is measured and used in RFP's in general and in MST in particular. Upon close scrutiny, the polynomial function model presently in use on MST is surprisingly good. Several small corrections could be made, but their implementation poses special problems and thus is probably not worth the effort at present. If we continue to reduce the loop voltage in MST, the corrections will become more important, and we may have to reconsider.

FIG. 1

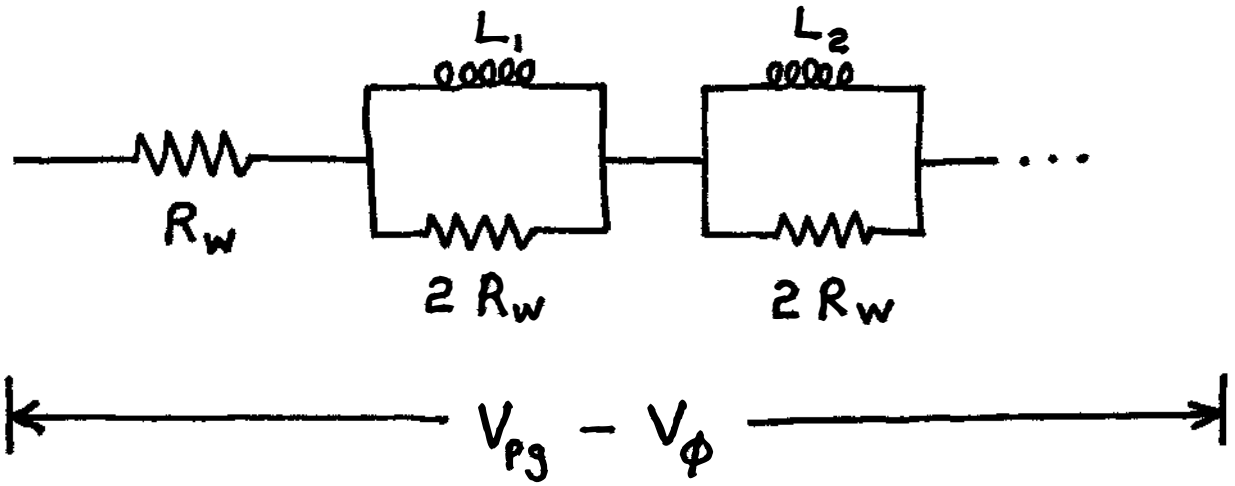

where $R_w = \frac{R_0 \rho}{a d}$ $(= 2.3\ \mu\Omega$ for MST)

$L_n = \frac{2 \mu_0 R_0 d}{\pi^2 a n^2}$ $(= 37/n^2$ nH for MST)

For MST, note:

$\rho = 4.0 \times 10^{-8}\ \Omega\text{-m}$

$R_0 = 1.5\ m$

$a = 0.52\ m$

$L_w = \sum_{n=1}^{\infty} L_n = 60\ nH$

FIG. 2

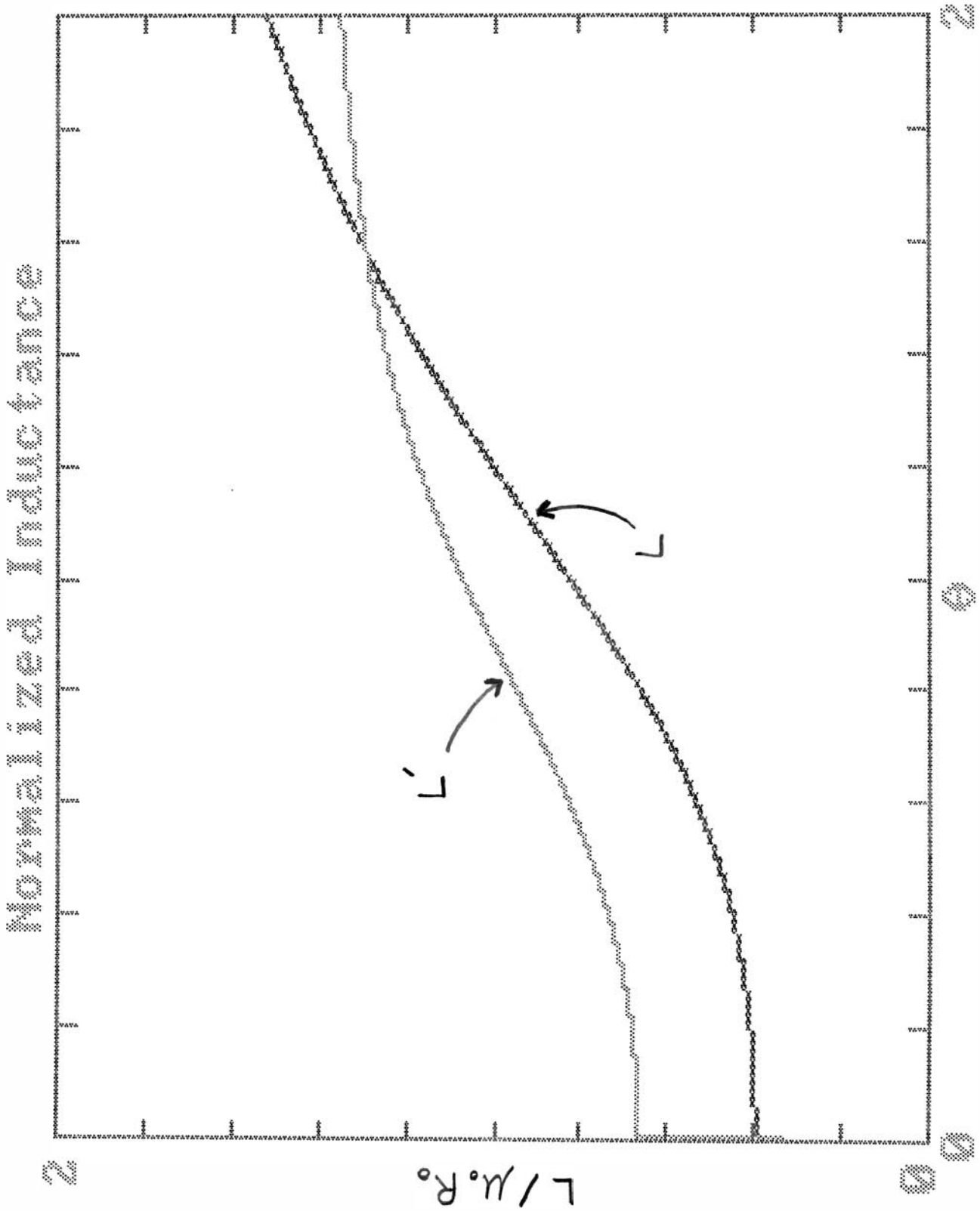

FIG. 3

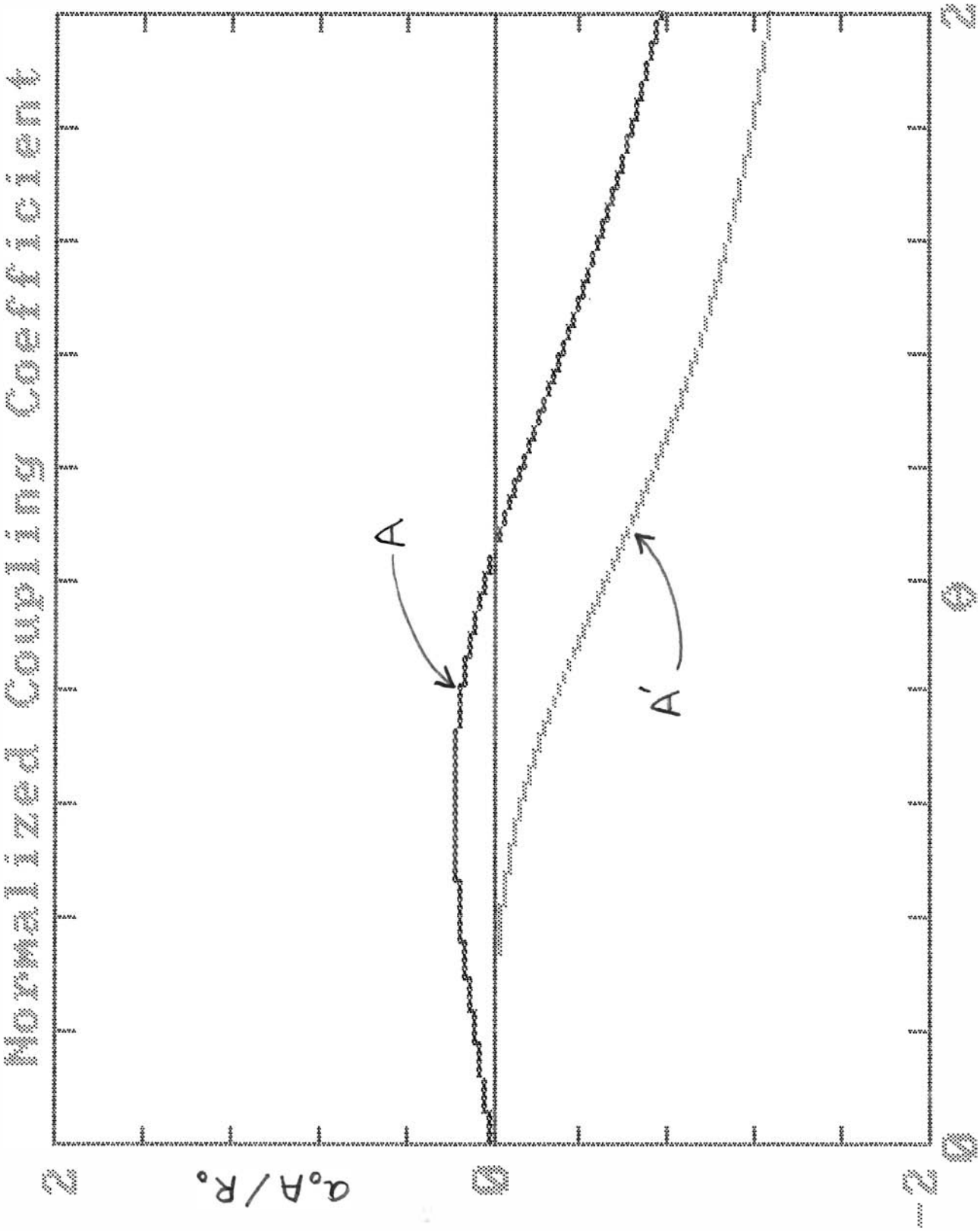

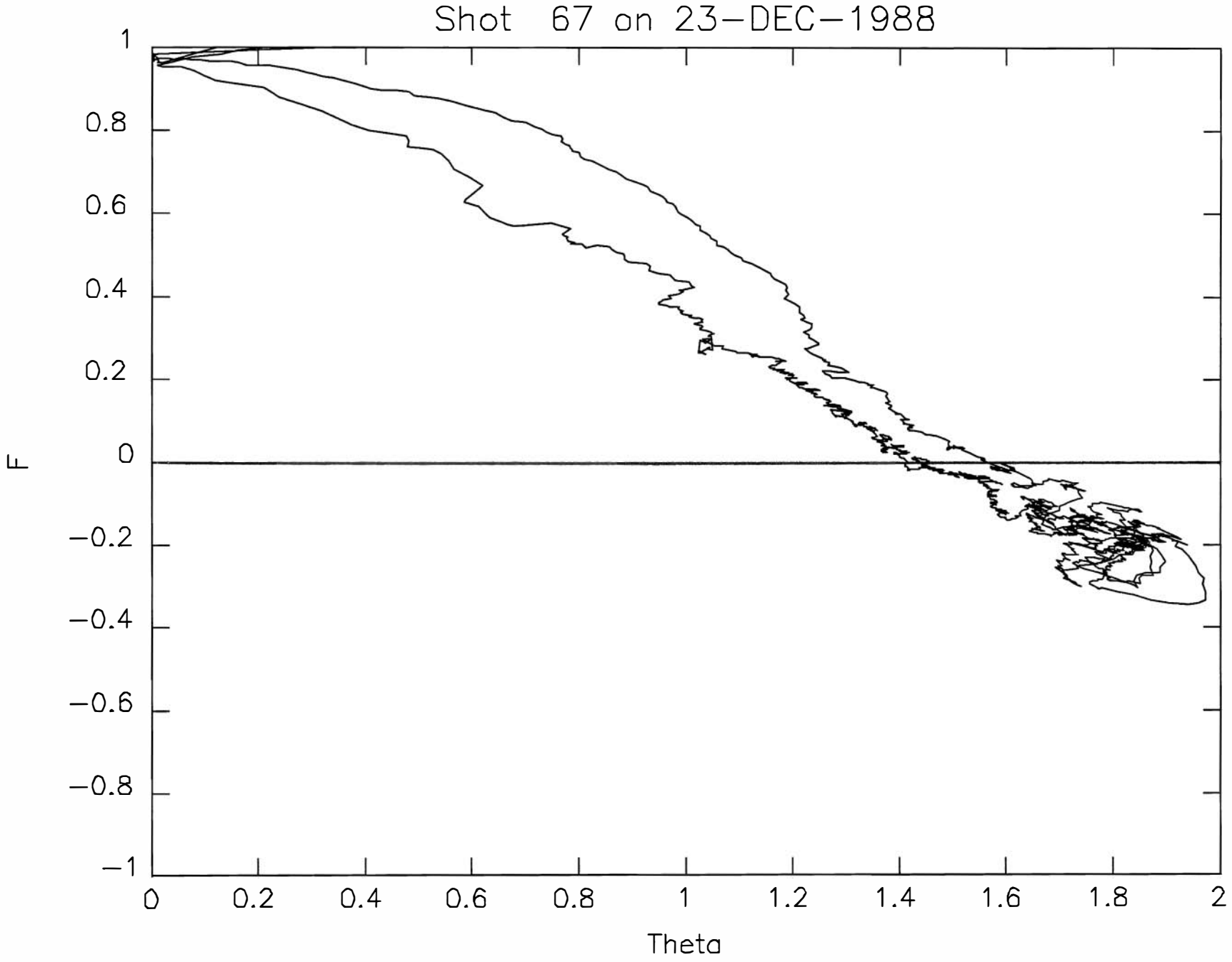
Shot 67 on 23-DEC-1988
F
Theta
1
0.8
0.6
0.4
0.2
0
−0.2
−0.4
−0.6
−0.8
−1
0
0.2
0.4
0.6
0.8
1
1.2
1.4
1.6
1.8
2

FIG. 4

FIG. 5

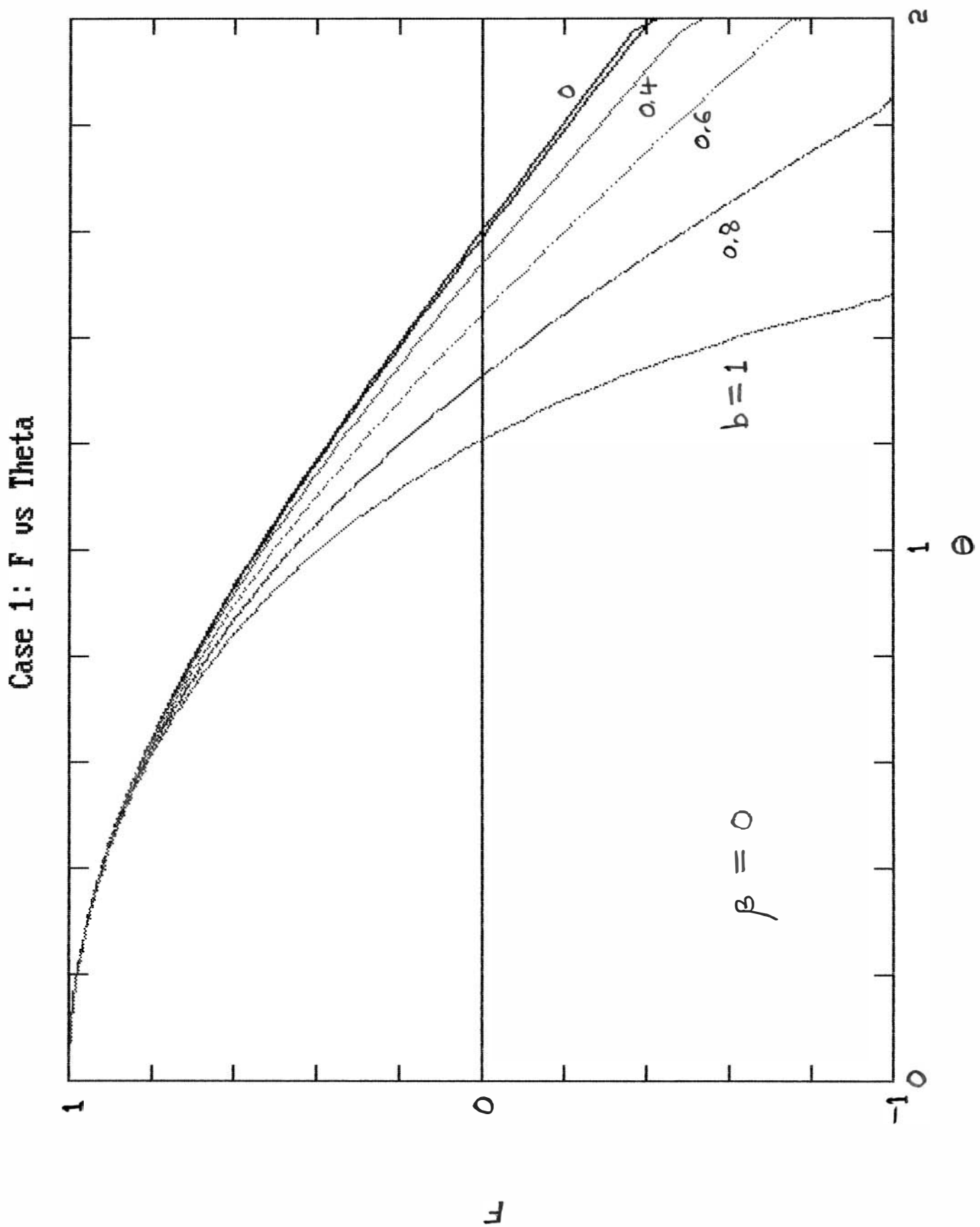

FIG. 6

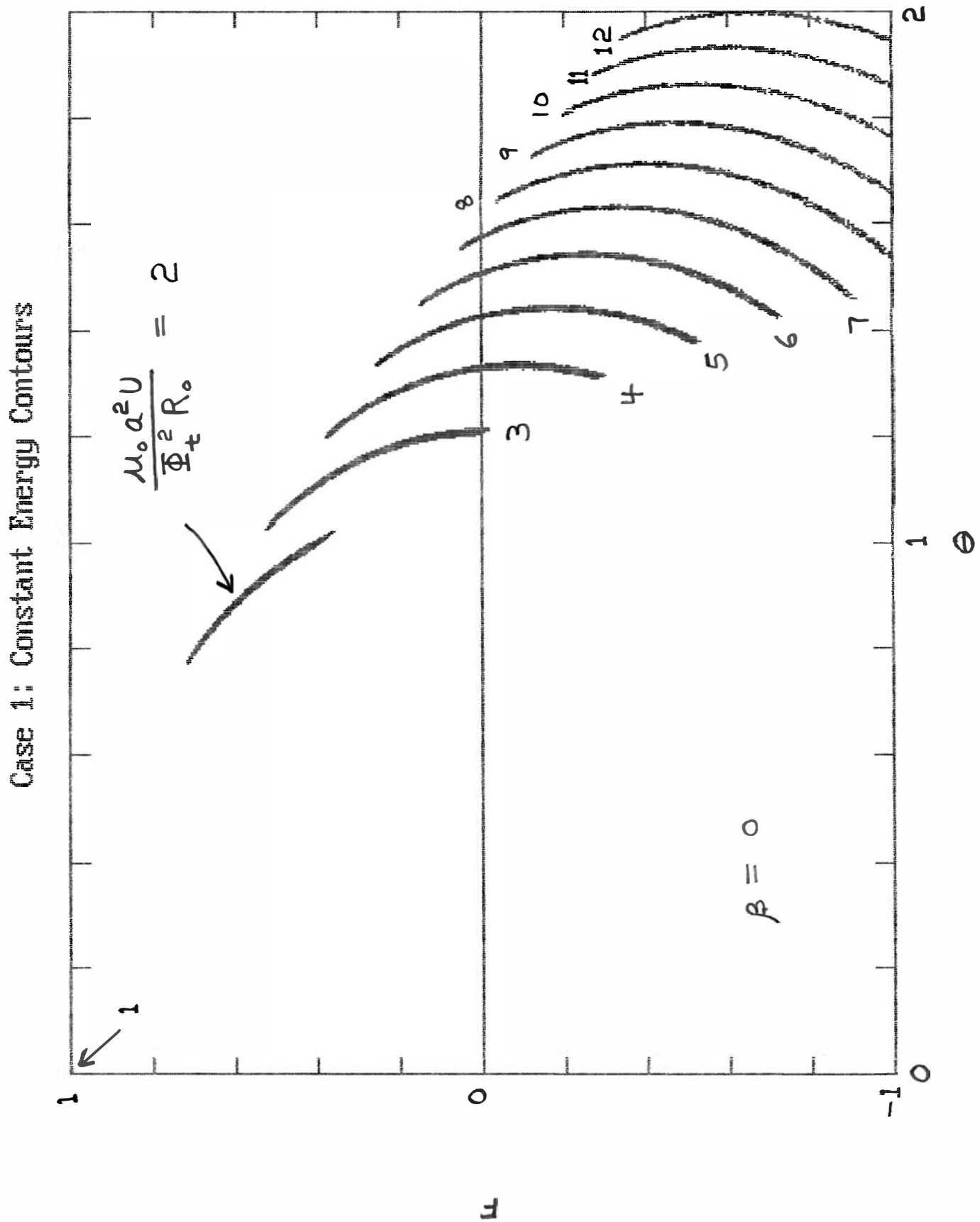
Case 1: Constant Energy Contours
$\frac{\mu_0 a^2 U}{\Phi_t^2 R_0} = 2$
3
4
5
6
7
8
9
10
11
12
1
$\beta = 0$
1
0
-1
0
1
2
r
θ

FIG. 7

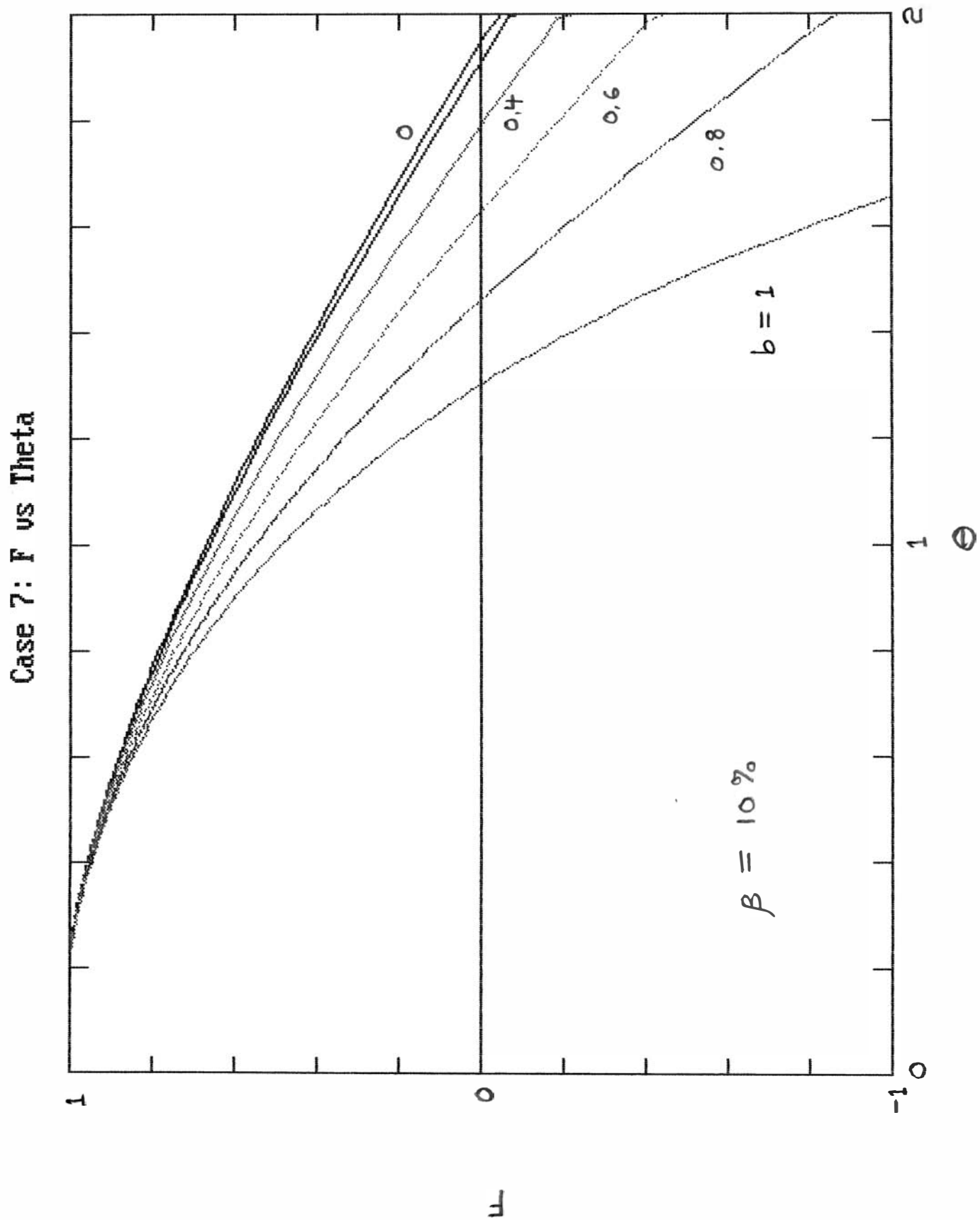

FIG. 8

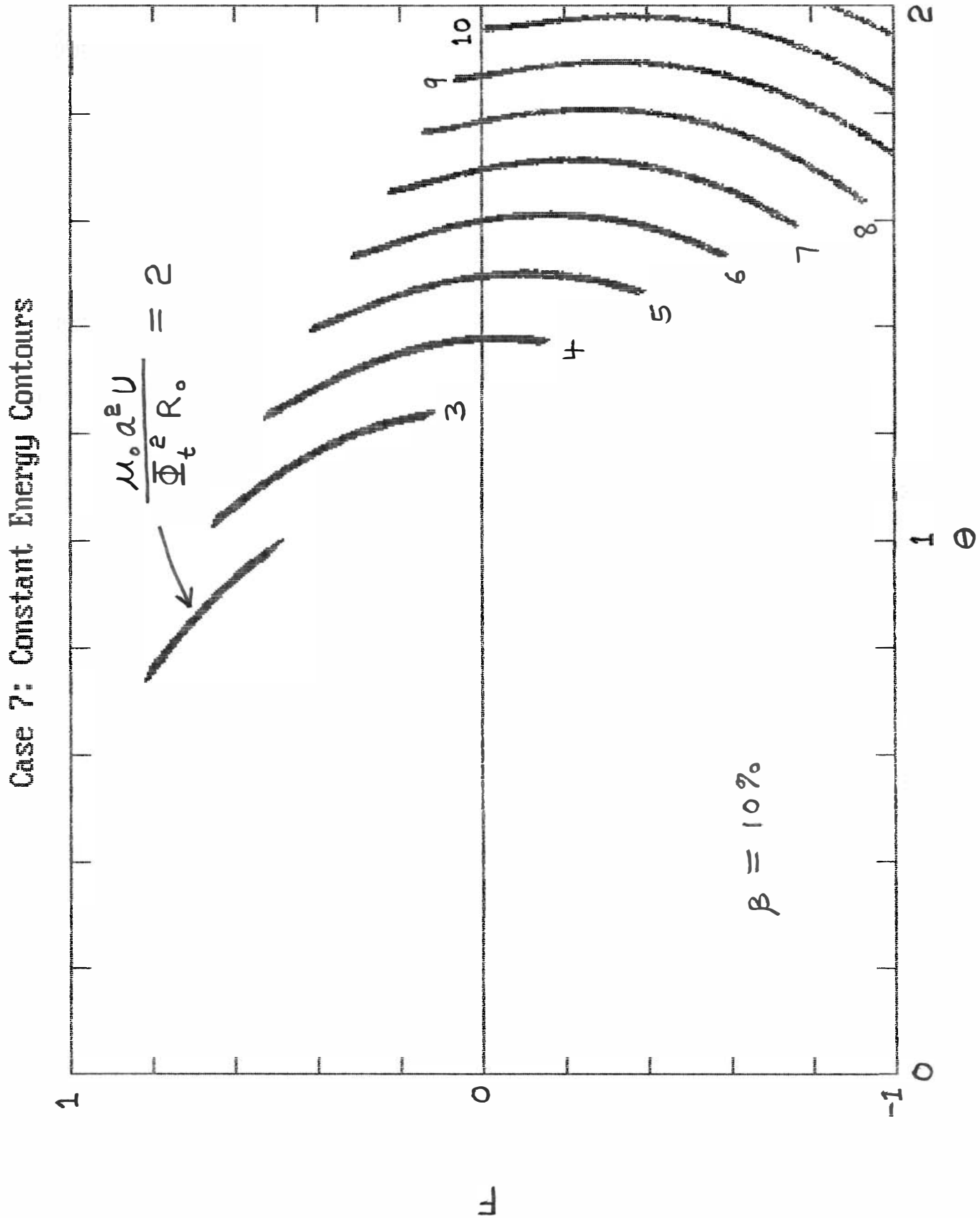
Case 7: Constant Energy Contours
$\frac{\mu_0 a^2 U}{\Phi_t^2 R_0} = 2$
3
4
5
6
7
8
9
10
$\beta = 10\%$
1
0
-1
0
1
2
Θ
Γ

FIG. 9

Total Energy

F	θ=0.0	0.2	0.4	0.6	0.8	1.0	1.2	1.4	1.6	1.8	2.0
1.0											
0.9											
0.8											
0.7					1.969						
0.6											
0.5						2.355					
0.4						1.922					
0.3							3.380				
0.2							3.052	5.325			
0.1							2.840	4.887			
-0.0								4.523	7.243		
-0.1								4.504	6.570		
-0.2								4.489	6.535	9.429	
-0.3								4.501	6.477	9.095	
-0.4								4.763	6.457	8.951	12.306
-0.5								5.032	6.681	8.864	11.972
-0.6								5.123	6.727	9.094	11.771
-0.7									7.063	9.112	11.805
-0.8									7.447	9.499	11.872
-0.9									7.839	9.733	12.159
-1.0									8.125	9.956	12.261

$$\frac{\mu_0 a^2 U}{\Phi_t^2 R_0}$$

Self Inductance

F	θ=0.0	0.2	0.4	0.6	0.8	1.0	1.2	1.4	1.6	1.8	2.0
1.0											
0.9											
0.8											
0.7					2.885						
0.6											
0.5						2.499					
0.4						1.944					
0.3							2.261				
0.2							1.860	2.880			
0.1							1.620	2.205			
-0.0								1.809	2.752		
-0.1								1.744	2.035		
-0.2								1.538	1.945	2.579	
-0.3								1.462	1.804	2.136	
-0.4								1.372	1.634	2.002	2.503
-0.5								1.291	1.529	1.827	2.199
-0.6								1.276	1.477	1.662	2.109
-0.7									1.420	1.621	1.829
-0.8									1.344	1.513	1.801
-0.9									1.303	1.471	1.633
-1.0									1.281	1.442	1.626

$$\frac{L''}{\mu_0 R_0}$$

FIG. 9 (con't)

Coupling Coefficient

F	θ=0.0	0.2	0.4	0.6	0.8	1.0	1.2	1.4	1.6	1.8	2.0
1.0											
0.9											
0.8											
0.7					-6.730						
0.6											
0.5						-4.639					
0.4						-2.956					
0.3							-3.402				
0.2							-2.252	-4.879			
0.1							-1.580	-2.880			
-0.0								-1.766	-4.219		
-0.1								-1.576	-2.146		
-0.2								-0.972	-1.886	-3.506	
-0.3								-0.744	-1.483	-2.221	
-0.4								-0.425	-0.996	-1.843	-3.115
-0.5								-0.125	-0.663	-1.346	-2.238
-0.6								-0.062	-0.503	-0.852	-1.988
-0.7									-0.293	-0.733	-1.182
-0.8									-0.012	-0.386	-1.097
-0.9									0.162	-0.239	-0.597
-1.0									0.268	-0.136	-0.570

$\frac{aA''}{R_o}$

Mutual Inductance

F	θ=0.0	0.2	0.4	0.6	0.8	1.0	1.2	1.4	1.6	1.8	2.0
1.0											
0.9											
0.8											
0.7					2.666						
0.6											
0.5						1.532					
0.4						0.765					
0.3							0.950				
0.2							0.463	1.429			
0.1							0.168	0.676			
-0.0								0.227	1.103		
-0.1								0.147	0.339		
-0.2								-0.113	0.237	0.786	
-0.3								-0.213	0.075	0.321	
-0.4								-0.358	-0.127	0.179	0.597
-0.5								-0.497	-0.271	-0.015	0.285
-0.6								-0.528	-0.342	-0.218	0.195
-0.7									-0.437	-0.267	-0.113
-0.8									-0.568	-0.418	-0.147
-0.9									-0.651	-0.483	-0.351
-1.0									-0.704	-0.531	-0.363

$\frac{M''}{\mu_o a}$

FIG. 10

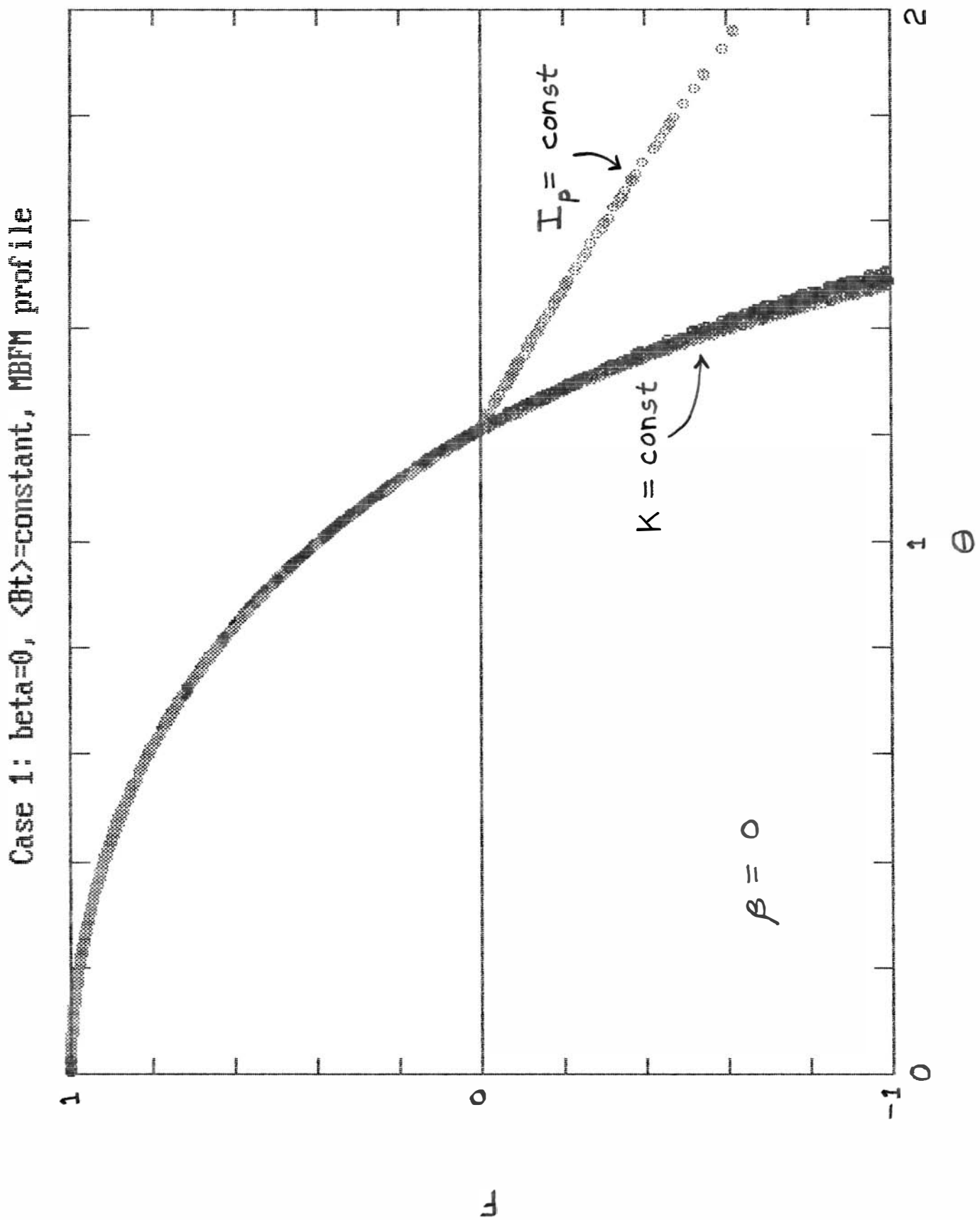
Case 1: beta=0, <Bt>=constant, MBFM profile
F
Θ
1
0
-1
0
1
2
I_p = const
K = const
β = 0

FIG. 11

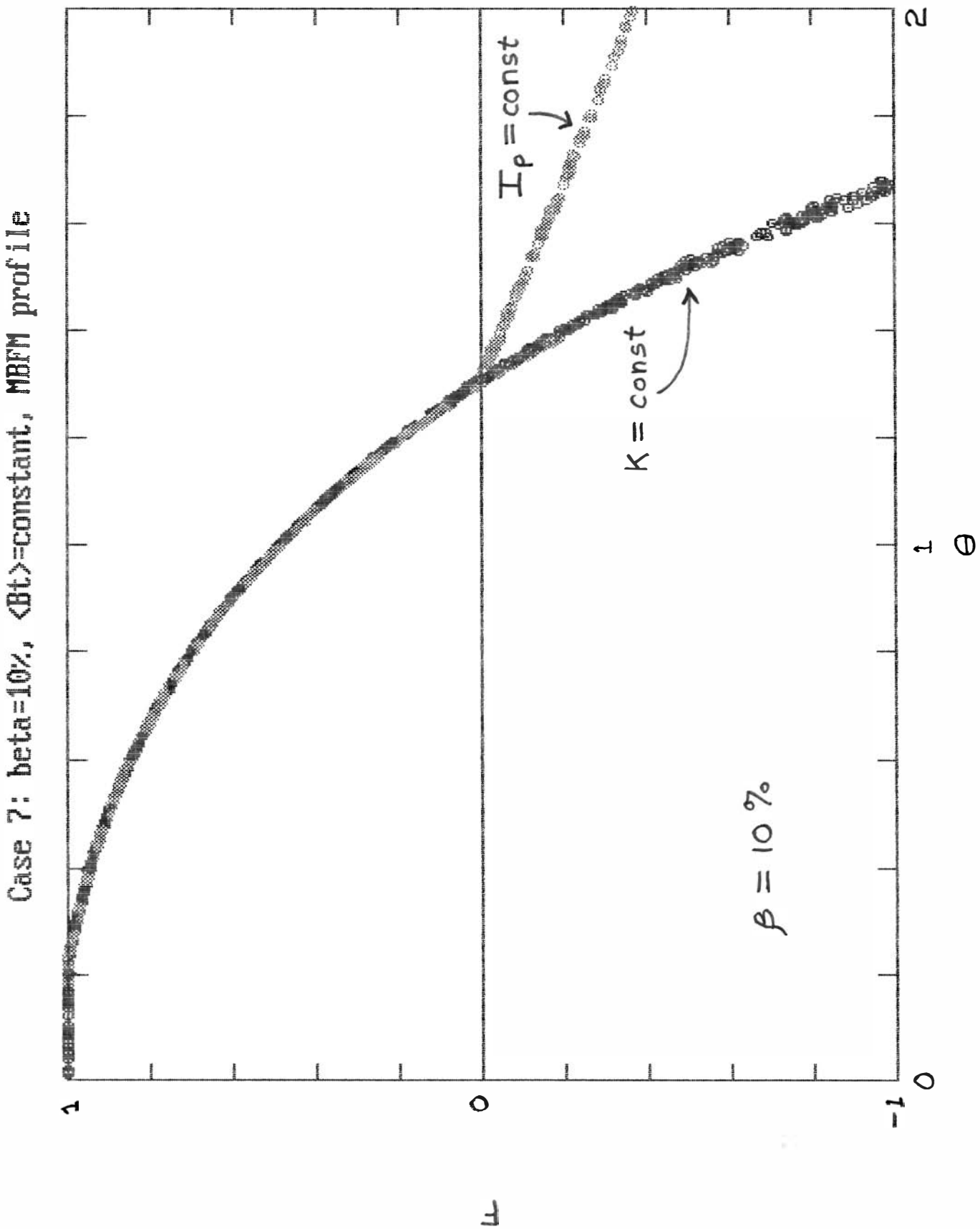
Case 7: beta=10%, <Bt>=constant, MBFM profile
I_p = const
K = const
β = 10 %
r
θ
1
0
-1
0
1
2